MODEL FOR THE RELATIONSHIP OF GRANULATION AND SUPERGRANULATION

V. KRISHAN
Indian Institute of Astrophysics

In this chapter a mechanism is proposed for producing the observed solar supergranulation from the photospheric granulation by a dissipative decay of two dimensional turbulence, which leads to concentration of the energy spectrum to the longest wavelengths. This concentration of convective eddies by selective dissipation to the scale with the maximum available spatial dimension and with a much longer time scale is verified by mode-mode coupling seen in computer simulations as well as in laboratory experiments. Theoretical predictions for these granulation scales and magnetic structures can be tested by high quality observations of the solar surface.

I. INTRODUCTION

Radiation and convection are the two main energy transport processes in the solar interior. The convective transport becomes operative where the temperature and density gradients are such that a fluid element, when displaced from its equilibrium position, keeps moving away from it. This stratification, through unstable convection, produces turbulence in the medium. The fluid eddies of varying sizes then carry energy as they propagate and dissipate. The cellular patterns observed on the solar surface are believed to be the manifestations of convective phenomena occurring in the subphotospheric layers. The cellular velocity fields are seen prominently on two scales: the granulation and the supergranulation, though mesogranulation and giant cells are also suspected to be present. The formation of granules with an average size of 1000 km and a life time of a few minutes can be understood either from the mixing length (Schwarzschild 1975) or from the linear instability (Bogart et al. 1980) description of the convection in the hydrogen ionization zone of the subphotospheric medium. The supergranules, with an average size of 30,000 km and a life time of 20 hr, do not have an unambiguous association with a subphotospheric region. Attempts have been made to identify this region and to seek an explanation for the energy concentration at the supergranular scale. Simon and Leighton (1964) suggested helium ionization to be responsible for accumulation of energy at supergranular scales. Convective modes with dominant growth rates at the two scales have been favored by Simon and Weiss (1968), Bogart et al. (1980) and Antia et al. (1984).

Here, a new mechanism of making supergranules is presented. It is based on the very special redistribution of the energy associated with the granules in a turbulent medium. Before discussing the particular processes that facilitate the formation of supergranules from granules, a few comments on the general properties of a turbulent medium are in order.

Formation of ordered structures in a turbulent medium relates to the concept of self-organization, which occurs when a system has two or more invariants in the absence of dissipation. The invariants suffer selective decay in the presence of dissipation. One conserved quantity has a higher decay rate than the others. The cascading process is such that the slowly decaying quantity transfers towards smaller wavenumber and thus appears in the form of a large-scale organized pattern. The system can be described using a variational principle where the fast decaying quantity is minimized keeping the slowly decaying quantity constant. Kraichnan (1967) found that in a two-dimensional hydrodynamic turbulence, the energy cascades toward large spatial scales and enstrophy, which is the total squared vorticity, and towards small spatial scales where it suffers heavy dissipation. It is this property of selective decay that facilitates the formation of large structures, whose dimensions are determined from the ratio of energy and enstrophy.

The condition of two dimensionality needs to be clarified. It is shown in the following sections that a velocity field $V = (V_x(x,y), V_y(x,y), V_z)$ with a constant vertical V_z component, and with the other two components varying only horizontally, satisfies the requirements of two-dimensional hydrodynamic turbulence. We shall call this the generalized "2-D" situation. The observed nearly two-dimensional velocity field associated with supergranules encourages us to investigate the role of 2-D hydrodynamic turbulence in the formation of supergranules. The inertial range of the turbulent spectrum is derived in Sec. II. Section III deals with the inverse cascade through mode-mode interaction. The concept of self-organization in 2-D turbulence is discussed in Sec. IV and a model of supergranulation is proposed in Sec. V. The inverse cascade in 3-D, and how a 3-D situation develops into a quasi 2-D one, are discussed in Sec. VI and finally the role of the magnetic field is addressed in Sec. VII.

II. THE INERTIAL RANGE OF THE TURBULENT SPECTRUM

The hydrodynamic equations describing the motion of an element in an incompressible fluid are:

$$\frac{d\mathbf{V}}{dt} = \frac{\partial \mathbf{V}}{\partial t} + (\mathbf{V} \cdot \nabla)\mathbf{V} = -\nabla T + \nu \nabla^2 \mathbf{V} \tag{1}$$

$$\nabla \cdot \mathbf{V} = 0. \tag{2}$$

Here $\mathbf{V}$ is the velocity, $T = p/\rho$ is a normalized temperature, p is pressure, ρ is density and ν is the kinematic viscosity. The equation for the vorticity vector Ω can be derived from Eqs. (1) and (2) as:

$$\frac{d\Omega}{dt} = \frac{\partial \Omega}{\partial t} + (\mathbf{V} \cdot \nabla)\Omega = \nu \nabla^2 \Omega \tag{3}$$

$$\Omega = \nabla \times \mathbf{V}. \tag{4}$$

In generalized 2-D, $\mathbf{V}$ and Ω may be expressed by a scalar stream function ψ as:

$$\mathbf{V} = -\nabla\psi \times \hat{z} + V_z \hat{z} \tag{5}$$

$$\Omega = \nabla^2 \psi \, \hat{z}. \tag{6}$$

Here $\hat{z}$ is a unit vector and V_z is the constant z-component of velocity $\mathbf{V}$. Equation (3) can be rewritten as:

$$\frac{\partial}{\partial t} \nabla^2 \psi \hat{z} + \{-\nabla\psi \times \hat{z} + V_z \hat{z}\} \cdot \nabla \{\nabla^2 \psi \hat{z}\} - \nu \nabla^4 \psi = 0 \tag{7}$$

where

$$\nabla \equiv \frac{\partial}{\partial x} \hat{x} + \frac{\partial}{\partial y} \hat{y}. \tag{8}$$

One notes that the term $(V_z \hat{z}) \cdot \nabla (\nabla^2 \psi \hat{z})$ vanishes for the generalized 2-D system. If the viscosity is small, i.e., the Reynolds number is large, the time evolution of the velocity field is determined by the second term in Eq. (7), which represents the coupling of various spatial fourier components in a turbulent state. The equation for mode coupling is obtained from Eq. (7) by expressing ψ as:

$$\psi = \tfrac{1}{2}\left[\sum_{k} \psi_K(t) \exp(i\,\mathbf{K}\cdot\mathbf{X}) + C.C.\right] \tag{9}$$

where **K** is a two-dimensional wave vector and ψ_K is the fourier amplitude. Equation (6) can be rewritten as:

$$\frac{\mathrm{d}\psi_K}{\mathrm{d}t} + K^2\nu\,\psi_K = \tfrac{1}{2} \sum_{K=K'+K''} \Lambda^{K}_{K'K''}\,\psi_{K'}\,\psi_{K''} \tag{10}$$

where

$$\Lambda^{K}_{K'K''} = \frac{1}{K^2}(\mathbf{K}' \times \mathbf{K}'')\cdot\hat{z}\,(K''^2 - K'^2). \tag{11}$$

The total energy W and the enstrophy U are defined as:

$$W = \tfrac{1}{2}\int V^2 \mathrm{d}^3r, \qquad U = \int \frac{\Omega^2}{2}\mathrm{d}^3r. \tag{12}$$

The conservation of energy and enstrophy in the absence of dissipation ($\nu = 0$) can be easily proved if the fluid is surrounded by either a periodic boundary or a rigid boundary, so that the normal component of the velocity vanishes on the boundary. Enstrophy conservation remains valid as long as the vorticity Ω is along $\hat{z}$ and $\mathbf{V}$ is in the (x, y) plane. Since there are two invariants, two types of inertial ranges are expected, one for energy and the other for enstrophy. These can be derived by using Kolmogorov arguments. The inertial range for energy is the well-known Kolmogorov law:

$$W(K) = C\left(\frac{\epsilon}{\rho}\right)^{2/3} K^{-5/3} \tag{13}$$

where ϵ is the dissipation rate of energy at a sink, C is a universal dimensionless constant, and $\int W(K)\mathrm{d}K$ gives the total energy. The enstrophy density is given by $K^2V_K^2$, and the inertial range for enstrophy requires that $(\rho K^2 V_K^2)(KV_K) = \epsilon' =$ constant. The energy spectrum in this range is given by:

$$W(K) = C'\left(\frac{\epsilon'}{\rho}\right)^{2/3} K^{-3}. \tag{14}$$

The range of validity of the two inertial ranges (Eqs. 13 and 14) can be established by investigating the cascading process (Sec. III).

III. INVERSE CASCADE THROUGH MODE-MODE COUPLING

Let there be a source at $K = K_S$ with energy W_S. Through mode-mode coupling, this would decay to two modes with wavenumbers K_1 and K_2. Since energy W and enstrophy U are conserved, one can calculate the energies W_1 and W_2 and enstrophies U_1 and U_2 of the modes K_1 and K_2 as (Hasegawa 1985):

$$\begin{aligned} W_S &= W_1 + W_2, \qquad U_S = U_1 + U_2 \\ K_S^2 W_S &= K_1^2 W_1 + K_2^2 W_2. \end{aligned} \tag{15}$$

From Eq. (15) one finds

$$\begin{aligned} W_1 &= \frac{K_2^2 - K_S^2}{K_2^2 - K_1^2} W_S, \qquad U_1 = K_1^2 W_1 \\ W_2 &= \frac{K_S^2 - K_1^2}{K_2^2 - K_1^2} W_S, \qquad U_2 = K_2^2 W_2. \end{aligned} \tag{16}$$

For $W_1, W_2 > 0$, $K_2^2 > K_S^2 > K_1^2$ should be satisfied. Thus K_S decays to two modes, one with wavenumber $K_1 < K_S$, and to another mode with $K_2 > K_S$. Hasegawa and Kodama (1978) have shown that the decay rate is maximum when:

$$\begin{aligned} p &= \frac{K_1^2}{K_S^2} = (\sqrt{2} - 1) \\ K_2^2 &= K_S^2 + K_1^2. \end{aligned} \tag{17}$$

Then

$$\begin{aligned} W_1 &= p\, W_S \qquad W_2 = (1-p) W_S, \\ U_1 &= p^2\, U_S, \qquad U_2 = (1-p^2) U_S. \end{aligned} \tag{18}$$

In the next step of the cascade, the mode at K_1^2 decays to modes at $pK_1^2 = p^2K_S^2$ and $(1+p)K_1^2 = p(1+p)K_S^2$. The mode at K_2 decays to modes at $pK_2^2 = p(1+p)K_S^2$ and $(1+p)K_2^2 = (1+p)^2K_S^2$. The corresponding energy partitions are p^2W_S, $2p(1-p)W_S$, and $(1-p)^2W_S$ for wavenumbers at $p^2K_S^2$, $p(1+p)K_S^2$, and $(1+p)K_S^2$, respectively. Continuing to the n[th] step, the energy distribution is given by a binomial distribution for a parameter (r/n) such that

$$W(K^2 = p^{n-r}(1+p)^r K_S^2) = {}^nC_r\, p^{n-r}(1-p)^r\, W_S. \tag{19}$$

Equation (19) gives the energy spectrum which results from a series of cascades at a fixed ratio $(K_l^2/K_s^2) = p$ at each step, where $K_l^2 + K_s^2 = K_2^2$. It can easily be shown that the energy spectrum condenses at $K \to 0$ as $n \to \infty$. Hence an inverse cascade and condensation of the spectrum at $K \to 0$ is expected from this model. Inverse cascade obtained this way is a consequence of conservation of energy and enstrophy.

IV. SELF-ORGANIZATION IN TWO-DIMENSIONAL TURBULENCE

Kraichnan's hypothesis of inverse cascade and inertial range spectra (Kraichnan 1967) has been tested by solving Eq. (10) numerically (Batchelor 1969; Lilly 1969; Fornberg 1977) as shown in Fig. 1. The creation of large-scale structures in the stream function in two-dimensional fluids has also been observed in laboratory experiments. The condensation of energy at the longest wavelengths permitted, due either to the finite size of the container or to the periodic boundary condition, has been reproduced in computer simulations (Hossain et al. 1983).

From modal transfer, it is clear that enstrophy cascades towards the shortest length scales and then suffers viscous dissipation. Thus, if the enstrophy $\int(\Omega^2/2)\,d^3r$ vanishes during normal cascade, the total energy W attains constancy even in the presence of viscosity. This, together with the experimental evidence for the inverse cascade, indicates that the system will

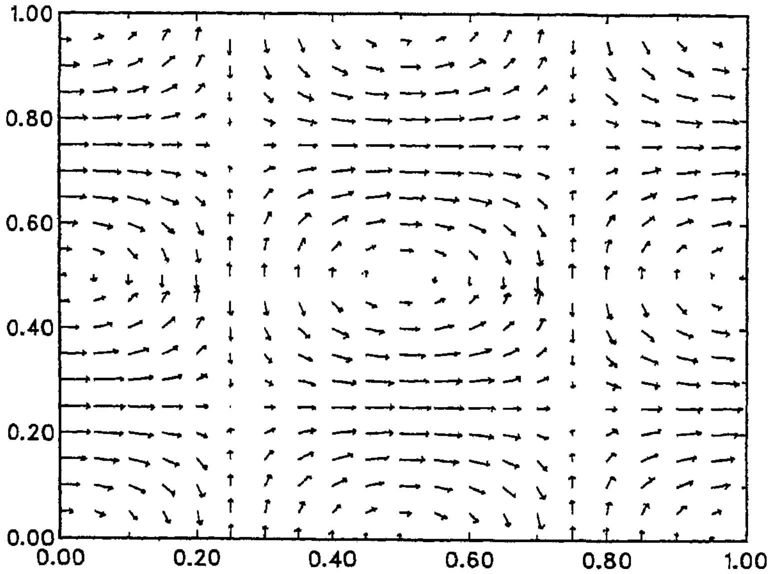

Fig. 1. Velocity field as calculated from Eq. (10).

evolve to a state of minimum enstrophy with constant energy. Such a dissipative process is called selective dissipation (Kraichnan and Montgomery 1980). Thus the large-scale structure appears as a result of minimization of enstrophy with the constraint of constant energy. This is expressed as

$$\delta U - \lambda\, \delta W = 0. \tag{20}$$

For periodic boundary conditions or for a viscous boundary such that $\Omega = 0$ at the boundary, one finds:

$$\nabla \times (\nabla \times \mathbf{V}) - \lambda\, \mathbf{V} = 0 \tag{21}$$

which can be solved by using the stream function that is determined by

$$\nabla^2\psi + \lambda\psi = 0. \tag{22}$$

Since λ gives the ratio of enstrophy to energy, Eq. (22) should be solved for the minimum eigenvalue λ. If the fluid has a periodic boundary condition with the periods a and b in the x and y directions, then

$$\psi = \psi_0 \cos\frac{2\pi x}{a} \cos\frac{2\pi y}{b}. \tag{23}$$

The self-organized state obtained here is also a stationary solution of the dynamical Eq. (1). Substituting Eq. (22) into Eq. (1) and setting $\partial V/\partial t = 0$ and $\nu = 0$, one gets

$$\nabla\left(\frac{V^2}{2} + T + \frac{\Omega^2}{2\lambda}\right) = 0. \tag{24}$$

This gives the temperature profile $T(x,y)$ shown in Fig. 2.

V. APPLICATION TO SOLAR SUPERGRANULATION

The observed nearly two-dimensional nature of the velocity field in the supergranules permits us to use the results of Secs. II, III and IV. Based on this, we would like to propose and test the following model for formation of supergranular cells on the solar surface:

1. The supergranulation is produced as a result of redistribution of energy associated with granulation.

2. The redistribution of energy takes place in a region with predominantly horizontal velocity fields, i.e., between the middle chromosphere and photosphere, below which the velocity field becomes three dimensional and isotropic.

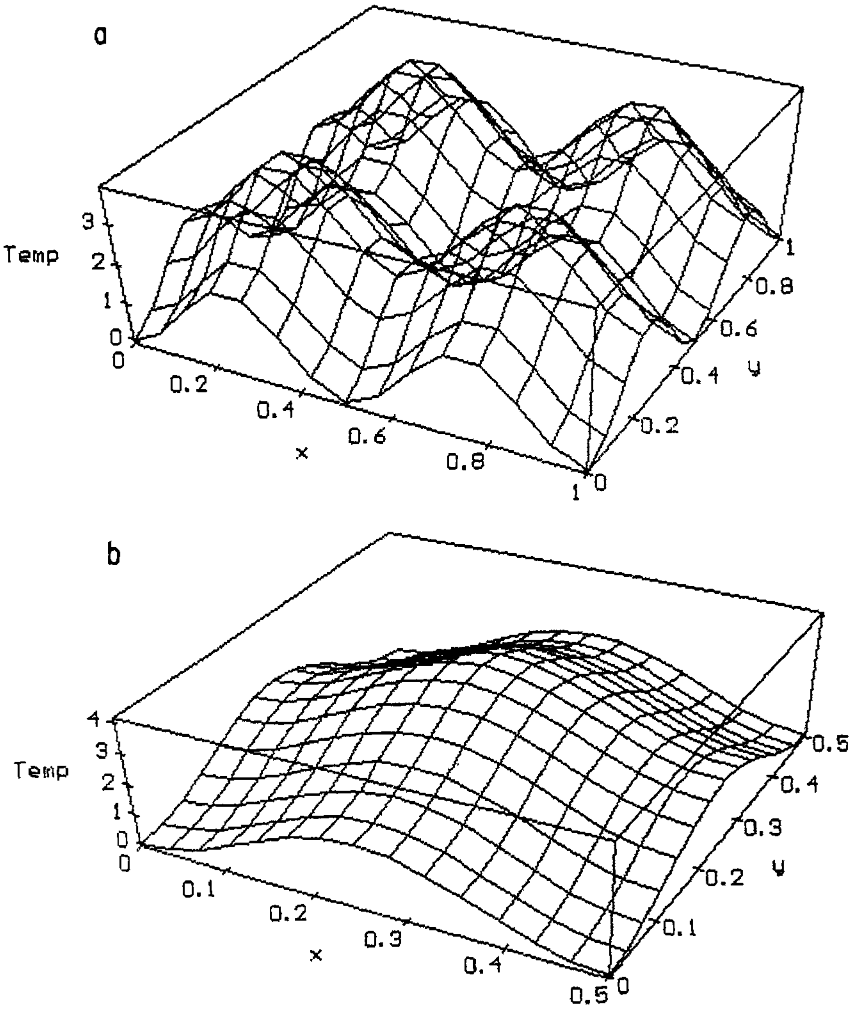

Fig. 2. Spatial distribution of temperature calculated from Eq. (23) in a region $(x/a, y/a) = (0,0)$ to $(1,1)$ plot (a) and $(0,0)$ to $(0.5,0.5)$ plot (b).

3. The redistribution of energy responsible for supergranulation occurs through the inverse cascade of energy towards larger scales, a consequence of the mode-mode interaction in a two-dimensional system with two invariants, the energy and the enstrophy.

4. The largest spatial scale is determined from the ratio of energy and enstrophy. From Eqs. (22) and (23), we find

$$\lambda = \left(\frac{2\pi}{a}\right)^2 + \left(\frac{2\pi}{b}\right)^2 \qquad (25)$$

where a and b are the dimensions of the organized structures, here the supergranular cell, and λ is the ratio of enstrophy U to energy W. Therefore, for $a \sim b \sim L$, the size of the cell, one finds

$$L = \left(\frac{8\pi^2}{\lambda}\right)^{1/2} = \left(\frac{8\pi^2 W}{U}\right)^{1/2}. \qquad (26)$$

For horizontal velocities $V \sim 0.5$ km s^{-1}, the energy per unit density and unit volume is $(1/2)(0.5\times 10^5)^2$ cm^2 s^{-2}. Therefore, to get $L \sim 30{,}000$ km, the value of enstrophy per unit density and unit volume is required to be 10^{-8} s^{-2}. It is instructive to compare this with the square of the average velocity gradient in the supergranular cell, i.e., with $(V/L)^2 \sim (0.5 \times 10^5/3 \times 10^9)^2 \sim 0.028 \times 10^{-8}$ s^{-2}. Thus, the required value of the enstrophy corresponds to a stronger velocity circulation.

5. The spatial variation of temperature within the supergranular cell is given by Eq. (24). For $a = b$, one finds $\partial T/\partial x$ is maximum at $(x = (2n+1)a/8, y)$ and $\partial T/\partial y$ is maximum at $(x, y = (2n+1)a/8)$.

6. The rate of modal transfer is given by the nonlinear term, and the associated time scale is $\sim(KV_K)^{-1}$. For the two inertial ranges one finds:

$$KV_K = K^{3/2}[W(K)]^{1/2} \propto K^{2/3} \text{ for } K < K_S \qquad (27)$$
$$\propto K^0 \text{ for } K > K_S.$$

Therefore, the characteristic time increases with the increase in the spatial scale, which means that the larger cells will have larger time scales.

7. The velocity field (V_x, V_y) given by Eq. (5) is plotted in Fig. 3 for the case $a = b$. The circulation pattern is clearly visible. This attains special significance in view of the recent observations of vortex formation in the granules (Brandt et al. 1988).

8. The distributions in energy and enstrophy would give a range of spatial scales, the largest of which may correspond to the giant cells.

Proposed tests of the model are the following:

A. If the energy input for supergranulation is at the granular scale K_S, then the energy spectrum should show a break at K_S: the spectrum should go as K^{-3} for $K > K_S$, and as $K^{-5/3}$ for $K < K_S$. Duvall (1987) has proposed two experiments to check the spectral behavior: (i) Doppler shift measurements, which have the advantage of providing a high-precision map of motions over the surface. The disadvantage is that one gets only one component of the horizontal motion, as the Doppler effect gives only the line-of-sight compo-

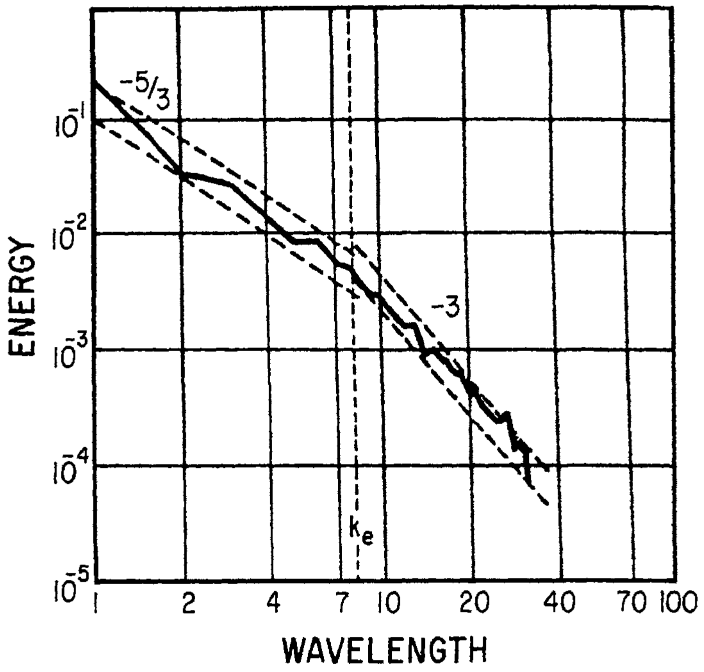

Fig. 3. An omnidirectional energy of two-dimensional Navier-Stokes turbulence obtained numerically (Lilly 1969). The initial spectrum dominated by the source spectrum at the source wave K_e, is shown to relax to the inertial range spectra for enstrophy at $K > K_e$ and energy at $K < K_e$.

nent; (ii) tracer measurements in which small magnetic elements can be followed and both horizontal components measured. The disadvantage is that one does not obtain a very dense grid of tracers, and this would yield a noisy measurement. Under the assumption that the two components of the horizontal motion are approximately equal, the Doppler method looks quite promising.

B. The constancy of energy and enstrophy can be verified with detailed observations of velocity fields.

C. The observed spatial variation of temperature when compared with the prediction of Eq. (23) will provide another test of this model.

VI. SOLAR GRANULATION AND 3-D HYDRODYNAMIC TURBULENCE

It has been shown in the previous sections that in a 2-D situation, the inverse cascade of energy can lead to the formation of large coherent structures, which in the case of the Sun may be the supergranular cells. But how good is the assumption of 2-D for the Sun? Levich (1985, and references therein) has shown that the inverse cascade occurs even in 3-D hydrodynamic turbulence. A qualitative description of this phenomenon, and investigation of the very important question of how a 3-D situation develops into a 2-D or a quasi 2-D one, are briefly attempted here. In analogy with the Earth's atmosphere (where the energy released is the latent heat of vaporization), the energy injection into the solar atmosphere occurs by convective upward motions, and the energy associated with the latent heat of ionization is released. It is estimated that 2 to 3% of the thermal energy is transferred into kinetic energy of random motions. This begs the question whether the excitation of random small-scale motions can lead to large organized structures that are observed in the form of granules, supergranules and even giant cells. Here, a picture that emphasizes the role of large helicity fluctuations in the cascading process is presented, as developed by Levich (1985) and co-workers for the formation of large cloud clusters, cyclones, and other related structures in the Earth's atmosphere. The helicity density, a measure of the knottedness of the vorticity field, is given by $\gamma = \mathbf{V}\cdot(\nabla \times \mathbf{V})$. A turbulent medium exhibits large fluctuations in helicity even though the mean helicity $< \mathbf{V}\cdot(\nabla \times \mathbf{V}) > = 0$. The reason for this is that in a nonequilibrium system, any quantity is expected to fluctuate strongly if there are no special restrictions. The fluctuating topology of the vorticity field in turbulent flows with $<\gamma> = 0$ is characterized by a statistical helicity invariant I, which represents the conserved mean square helicity per unit volume:

$$I = \lim_{V\to\infty} \frac{1}{V} \left\langle \left(\int \mathbf{V}\cdot\mathbf{\Omega} d^3r \right)^2 \right\rangle \propto \int [W(K)]^2 dK \qquad (28)$$

which is a constant for a nondissipative system. One recalls that the nonlinear term in the Navier-Stokes equation is $\nabla \times (\mathbf{V} \times \mathbf{\Omega})$. Thus if in some volume I is large, i.e., $(\mathbf{V}\cdot\mathbf{\Omega})$ is large, then $(\mathbf{V} \times \mathbf{\Omega})$ is very small. In other words, if $\mathbf{V}$ and $\mathbf{\Omega}$ are strongly aligned, the nonlinear interaction term is vanishingly small. Therefore the energy cascade to small scales is inhibited in this volume. Using Kolmogorov arguments (see Sec. II), one can determine the inertial range of the I invariant. If one substitutes $W(K) \propto K^{-5/3}$, which is the inertial range for energy in 3-D, into Eq. (28), one finds total energy $E = \int W(K) dK \propto L^{2/3}$ and $I \propto L^{7/3}$. Therefore, as was argued in the 2-D case, it is not possible to have both E and I conserved in the identical inertial range. Thus energy (like enstrophy in 2-D with larger K dependence) cascades to smaller scales and I to larger scales. It is more appropriate to say that the correlation length of helicity fluctuations increases, without carrying much energy with it. In the case of highly anisotropic flow, with the vertical scale $L_z << L_H$, the horizontal scale, as well as $V_z << V_x, V_y$, one gets

$$\frac{\mathrm{D}}{\mathrm{D}t} V_z = \frac{\partial V_z}{\partial t} + \left(V_x \frac{\partial}{\partial x} + V_y \frac{\partial}{\partial y}\right) V_z = 0 \tag{29}$$

i.e., V_z is convected by the horizontal velocity field. Therefore $<V_z^2>$ is ~ constant and independent of (x, y), which was previously called "generalized 2-D." The helicity density can be approximated as $V_x\Omega_x \sim V_y\Omega_y << V_z\Omega_z$. Then

$$\begin{aligned} I &= \int \langle (V_z\Omega_z)^2 \rangle \, \mathrm{d}x\mathrm{d}y\mathrm{d}z \propto z_0 \int \langle (V_z\Omega_z)^2 \rangle \, \mathrm{d}x\mathrm{d}y \\ &= z_0 \langle V_z^2 \rangle \int \langle \Omega_z^2 \rangle \, \mathrm{d}x\mathrm{d}y \propto L^{2/3} \end{aligned} \tag{30}$$

and from $\int I(K)\mathrm{d}K = I$, $I(K) \propto K^{-5/3}$, where L is the largest characteristic scale in the (x, y) plane. Thus the $I(K)$ spectrum coincides with the energy spectrum of 2-D turbulence, $W(K) \propto K^{-5/3}$, corresponding to the inverse cascade. Thus, the cascade of the I invariant to large scales is indistinguishable from that of the energy, in contrast to the fully 3-D case where a small energy flux accompanies the cascade of the I invariant. Intermediate situations correspond to various degrees of anisotropy. As anisotropy increases, the fraction of energy transferred to larger scales also increases. These conclusions can be summarized as:

(a) An anisotropic situation can develop from a completely isotropic one if the growth in the vertical direction is restricted due to some condition in the atmosphere. For example, in the solar photosphere this maximum vertical extent may be limited by the size of the region in which the temperature gradient remains superadiabatic.

(b) In the initial stages when isotropy dominates, most of the energy cascades to small scales where it suffers viscous dissipation. The cascade of the I invariant results in an increase of the correlation length of helicity fluctuations.

(c) When this correlation length becomes equal to the vertical scale imposed by requiring superadiabaticity, for example, the correlation can grow only in the horizontal plane. This gives rise to anisotropy.

(d) The anisotropic fluctuations act as a new anisotropic stirring force accompanied by increasing amounts of energy transfer to large scales.

(e) As the anisotropy grows, it facilitates the accumulation of energy at larger scales and thus the formation of large structures like supergranular cells.

(f) The growth of large structures in the case of anisotropic turbulence can again be interrupted as a result of symmetry braking for example, caused by the Coriolis force. At the length scale L_c where the nonlinear term of the Navier-Stokes equation becomes comparable to the Coriolis force, the inverse cascade is inhibited. In the quasi 2-D situation that exists, the Coriolis force, together with a lack of reflectional symmetry with respect to the horizontal plane, favors helical structures with a definite sign of helicity. It is found that in quasi 2-D, the Coriolis force favors cyclonic circulation, and the sign of helicity corresponding to the updraft cyclonic motion can be fixed. If downward motion is present, it must be anticyclonic to retain the same sign of helicity. It is also found that much greater energy is needed to maintain coherent structures at the scale L_c.

There are several related questions of the energetics, the life times, and the temporal evolution of these structures which need a detailed investigation (keeping in view the available observations of solar granulation), and which may give direction to what more needs to be measured about solar granulation.

VII. ROLE OF MAGNETIC FIELD

The enhancement of magnetic field at the supergranular cell boundaries due to horizontal motion has been discussed by Simon and Leighton (1964), where the maximum magnetic field builds up to the equipartition value. In the chromosphere the ratio of magnetic to kinetic energy is found to be greater than unity. The nature of magnetohydrodynamic turbulence in the presence of a strong magnetic field changes significantly (Montgomery and Turner 1981). The turbulent spectrum results from the interplay of three effects: (1) the driving mechanism; (2) dissipative mechanisms; and (3) the modal transfer due to nonlinear interaction between various spatial modes. From laboratory studies, it is found that in the presence of a strong magnetic field **B**, anisotropy is set up and the turbulent spectrum splits into two parts: (1) two-dimensional magnetohydrodynamic fluctuations carrying most of the energy in a plane perpendicular to the mean field $\mathbf{B}_0$; and (2) a more isotropic spectrum which is identified with Alfvén waves. In two-dimensional incompressible MHD, the square of the vector potential A^2 and the magnetic field **B** take the roles of V and Ω in two-dimensional Navier-Stokes turbulence. Thus an inverse cascade in the spectrum of A^2 can lead to an organized state such that

$$\delta \int (\nabla \times \mathbf{A})^2 \, dV - \lambda \delta \int A^2 dV = 0 \tag{31}$$

which gives

$$\nabla^2 \mathbf{A} + \lambda \mathbf{A} = 0. \tag{32}$$

The constant-A contours correspond to the magnetic lines of force, and the expected self-organized state is a pair of long wavelength circular magnetic fields. The cascade of A^2 to small wavenumbers and of magnetic field energy to large wavenumbers has been demonstrated by Pouquet (1978). The time scales of the 2-D MHD fluctuations are governed by nonlinear terms, whereas for the isotropic part these are the Alfvénic time scales. The Alfvénic part of the turbulent spectrum can be associated with the spicules, which Osterbrock (1961) described as slow-mode disturbances carrying chromospheric material up along the magnetic lines of force into the corona. The organized two-dimensional MHD turbulence could be an explanation for the formation of the magnetic network.

The predictions of the above model can be tested by measuring the correlation lengths along the mean field $\mathbf{B}_0$ and perpendicular to it. One expects that the correlation lengths along $\mathbf{B}_0$ are much longer than those transverse to $\mathbf{B}_0$. This is true for velocity and magnetic field fluctuations. The root-mean-square values of the transverse magnetic fluctuations are much larger than the longitudinal (along $\mathbf{B}_0$) fluctuations. The single-point frequency measurements for both magnetic and velocity field fluctuations are expected to show steep power-law frequency spectra that are negligibly small for frequencies below either the ion gyrofrequency or the ratio of the Alfvén speed to the correlation length, thus indicating the weakness of the higher-frequency Alfvénic spectrum.

The organizational properties of three-dimensional magnetohydrodynamic turbulence have been successfully used to delineate the structure of coronal loops (Krishan 1985*a,b*). The lowest-energy state emerges as a force-free state which reproduces the observed spatial variations of pressure in the coronal loops. In 3-D MHD, the new invariant, magnetic helicity, turns out to be a useful indicator of the pre-flare configuration of a flaring loop, as it is conjectured that during a flare, a high-energy, nearly force-free state decays to the lowest-energy state with the release of magnetic energy, while the magnetic helicity (due to inverse cascade) remains nearly constant (Krishan 1986).

Thus, these studies indicate the relevance and the resourcefulness of the concept of self-organization in magnetohydrodynamic turbulence in the solar context.

VIII. CONCLUSIONS

The inverse cascade of energy in two-dimensional hydrodynamic turbulence favors the formation of large organized structures. Application of this idea to the production of supergranulation seems to account for the observed spatial scale of the cellular motion. With inclusion of a strong magnetic field, for example, for the conditions obtained in the chromosphere, the turbulent spectrum consists of two parts: (1) anisotropic two-dimensional MHD fluctuations in the transverse direction; and (2) an Alfvénic spectrum along $\mathbf{B}_0$. The predictions about correlation lengths in the two directions along and perpendicular to $\mathbf{B}_0$ need to be tested by obtaining high-quality observations.

Acknowledgments. The author is grateful to D. Ter Haar for introducing her to the works of E. Levich and collaborators. Figure 3 has been reproduced from Hasegawa (1985).